Vol 16 No 3, March 2007
1009-1963/2007/16(03)/0788-07

Chinese Physics

© 2007 Chin. Phys. Soc.
and IOP Publishing Ltd

Composition-induced structural modifications in the quaternary $CuIn_{1-x}Ga_xSe_2$ thin films: bond properties versus Ga content*

Xu Chuan-Ming(徐传明)[a)†], Sun Yun(孙 云)[a)],
Li Feng-Yan(李凤岩)[a)], Zhang Li(张 力)[a)],
Xue Yu-Ming(薛玉明)[a)], He Qing(何 青)[a)], and Liu Hong-Tu(刘洪图)[b)]

[a)] *Institute of Photoelectronics, Nankai University, Tianjin* 300071, *China*

[b)] *Department of Physics, University of Science and Technology of China, Hefei* 230026, *China*

(Received 23 January 2006; revised manuscript received 10 July 2006)

In this paper the dependence of structural properties of the quaternary $CuIn_{1-x}Ga_xSe_2$ films with tetragonal structure on the Ga content has been systematically investigated by Raman scattering and x-ray diffraction spectra. The shift of the dominant A_1 mode, unlike the lattice constants, does not follow the linear Vegard law with increasing Ga content x, whereas exhibits approximately polynomial change from 174 cm^{-1} for $CuInSe_2$ to 185 cm^{-1} for $CuGaSe_2$. Such behaviour should be indicative of presence of the asymmetric distribution of Ga and In on a microscopic scale in the films, due to Ga addition. The changes in the tetragonal distortion η lead to a significant variation in the anion displacement parameter U, which should be responsible for the evolution of bond parameters and resultant Raman bands with x.

Keywords: chalcopyrite compounds, $CuIn_{1-x}Ga_xSe_2$ films, anion displacement, Raman scattering
PACC: 6160, 6860, 7830

1. Introduction

Solar cells based on quaternary polycrystalline $CuIn_{1-x}Ga_xSe_2$ (CIGS) absorbers, with the efficiencies approaching nearly 20%,[1] are highly successful among thin-film photovoltaic devices. These materials crystallize in the chalcopyrite structure like $A^IB^{III}C_2^{VI}$ type ($I\bar{4}2d$ space group), and their smallest units with energy minimization are A_2B_2 type of local tetrahedral cationic clusters around C, with generally unequal nearest-neighbour bond lengths $R_{A-C} \neq R_{B-C}$.[2,3] When In is substituted by the smaller atom Ga, the lattice compression should result in remarkable change in bond properties of CIGS materials, accompanied by notable displacement of the Se atoms which preserve the tetragonal structure. Raman spectroscopy has been used as a promising tool for the structural characterization of ternary $CuInSe_2$, $CuGaSe_2$[4−7] and quaternary CIGS[8−10] compounds by means of a shift of phonon frequencies. However, there are still many unclear phenomena in Raman spectra of CIGS, such as the effect of Ga addition on vibrational properties. For CIGS bulks crystal,[9,10] it shows that the dominant A_1 mode shifts toward higher wave numbers in linear curve as increasing x value, while the intensities of A_1 modes remain practically constant. For CIGS films, however, polycrystalline nature makes structural properties more complicated than that of their crystalline counterparts. The spontaneous formation of charge-neutral defect pair ($2V_{Cu}^- + In_{Cu}^{2+}/Ga^{2+}$)[3,11] enables the surface and bulk regions to tolerate many structural defects, i.e., cation vacancies, interstitials and antisites, by self-adjustment of their local chemistry and structure, even in nominal stoichiometric CIGS compounds.[5] As a result, actual films are highly nonstoichiometric on a microscopic scale,[1,12] and contain chemical fluctuation-induced nanodomains,[13] which result in the different local environment and cationic clusters in crystal structures. Thus, in such materials, the interaction between local clusters should change the bond properties in the lattice, and such effect will reflect on Raman spectra of CIGS films. In our preliminary study,[8] we found that the shift of A_1 band varies

*Project supported by China Postdoctoral Science Foundation (Grant No 2005037539), and the National High-Tech Research and Development Programm of China (Grant No 2004AA513020).
†E-mail: cmxu@ustc.edu

slightly in the films with $x = 0.3$. To our knowledge, no data on lattice vibration properties of quaternary CIGS films have been reported yet. Therefore, a further understanding of Ga effects on structural properties of CIGS is important both for studies of these materials and for the optimization of device performance.

In this paper, we systematically investigate the effects of Ga addition to $CuInSe_2$ on its structural properties by Raman spectroscopy and x-ray diffraction (XRD) spectra. Considering the complex defect situation and its dependence on the specific deviation from stoichiometry in the films,[1,3,6] on a macroscopic scale, we calculate the bond parameters of the lattice as a function of Ga content x and explain the composition-induced structural modifications in quaternary CIGS films.

2. Experimental details

The CIGS films with Ga content $x = 0$, 0.3, 0.5, 0.7 and 1.0 investigated were grown on the cleaned Na-free glass substrates by the periodical sequential evaporation method (i.e., forming In/Ga/Cu/In $\cdots$ for $0 < x < 1$ and Ga/Cu/Ga $\cdots$ for $x = 1$ stacking sequence) and subsequently vacuum-selenized annealing process with substrate temperature at 673 K for 3 hours.[8] The chemical composition of all the stoichiometric films with nominal 60 nm thickness obtained was confirmed by a XRF-1800 x-ray fluorescence spectrometer with Rh-anode. On the other hand, the films were examined by Philips X Pert PRO SUPER diffractometer with Cu Kα radiation. The unpolarized Raman spectra were recorded within the spectral resolution of 1 cm^{-1} at room temperature by using LABRAM-HR equipment and a 514.53 nm Ar^+ laser. The samples were measured twice to improve the signal-to-noise ratio.

3. Results and discussion

3.1. Structural studies

The XRD spectra of $CuIn_{1-x}Ga_xSe_2$ films are depicted as a function x in Fig.1. The relative intensities between the (112) peak and the (220)/(204) peak in the films, as an indicator of the correlations between chemical composition and the preferred orientation, are determined by calculating the areas under the diffraction peaks with Lorenzian fit (shown in the insert of Fig.1).

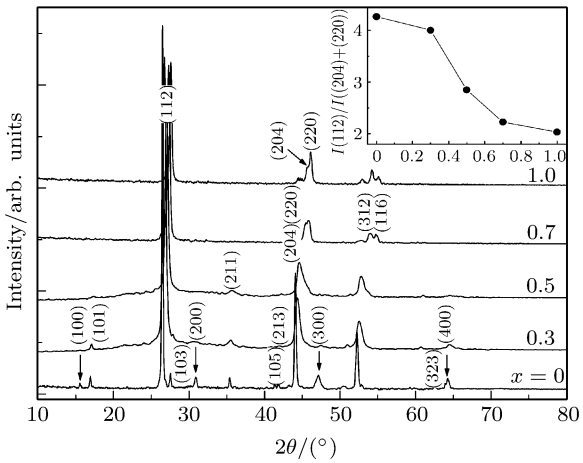


Fig.1. The composition dependence of XRD spectra of $CuIn_{1-x}Ga_xSe_2$ films. The inset shows the relative intensities between (112) and (204)/(220) peaks for the films.

From the XRD analysis, all the films in this work grow mainly with chalcopyrite structure, and along (112) preferred orientation. It is obviously found that the (112), (220)/(204) and (312)/(116) peaks shift toward higher angles as increasing x from $CuInSe_2$ to $CuGaSe_2$, which indicates the reduction of lattice constants, meanwhile, these lines observed in low-Ga films, i.e. (101), (103) and (211) disappear in the noise as $x \geq 0.5$, accompanied by intensity decrease of (112) peak and the splittings of the doublets (220)/(204) and (312)/(116). Such behaviour of the intensity changes in these peaks should be correlated to the formation of defect pair $(2V_{Cu}^{-} + In_{Cu}^{2+}/Ga_{Cu}^{2+})$ and resultant decomposition from nonpolar (220) surfaces to polar {112} facets.[14] Additionally, the intensity decrease of (103) reflection can be viewed as an indicator of the enhancement of (220) orientation.[15] It shows that the formation of a large number of more deeper donor Ga_{Cu} in the films with $x \geq 0.3$, in contrast to In_{Cu} in $CuInSe_2$, lowers the relative stability of the defect pairs,[11] which results in the intensity increase of (220) peak relative to (112) peak. On the other hand, four extra diffraction peaks observed in $CuInSe_2$, namely (100), (200), (300) and (400), become almost indiscernible in the noise with $x \geq 0.3$. These odd-integer peaks, in particular for (100) and (300), have been demonstrated as an indication of the presence of CuAu-ordered structure phases ($P\bar{4}m2$ space group)[5,6,16,17] which exhibits the same type

of A_2B_2 clusters,[3,18] in nominal chalcopyrite-ordered $CuInSe_2$ films. According to the evolution of such odd-integer reflections in Fig.1, it is expected that Ga addition could inhibit formation of the CuAu-ordered $CuInSe_2$, due to the fact that the formation energy of CuAu-ordered phase is rather smaller in $CuInSe_2$ than in $CuGaSe_2$,[18,19] which will be further verified later by Raman spectra.

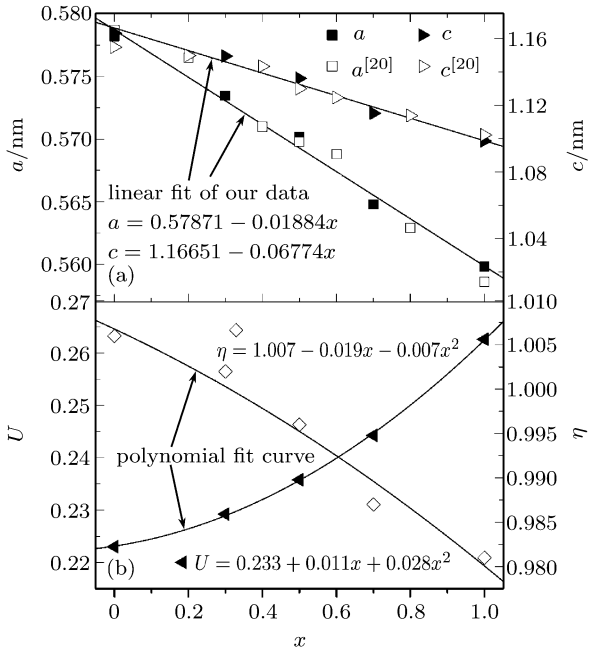


Fig.2. The values of the calculated structural parameters as a function of Ga content x: (a) lattice constants a and c; (b) anion displacement U and tetragonal distortion η.

Based on the XRD spectra of CIGS films in Fig.1, The calculated lattice constants a and c with x changing, which may give the tetragonal distortion value $\eta = c/2a$, are shown in Fig.2. The values of the a and c are obtained as 0.5721, 1.1635 nm for $CuInSe_2$, and 0.5598, 1.0981 nm for $CuGaSe_2$, respectively, being very close to the published results of their crystalline counterparts.[6,20,21] Moreover, it is clearly found that the a and c follow the usual linear Vegard behaviour over the whole x range, respectively, which can be delineated by the fitting curves in Fig.2(a), meantime, the η values decrease in approximately quadratic curve from 1.006 for $CuInSe_2$ to 0.981 for $CuGaSe_2$, as shown in Fig.2(b). For the films with $x \geq 0.5$, the $\eta < 1$ indicates the tetragonal compression which should be responsible for the splittings of the (220)/(204) and (312)/(116) pairs observed in Fig.1. Also, for the CuAu-ordered phase in $CuInSe_2$, the values of lattice parameters $a = 0.4086$ nm, $c = 0.57989$ nm are calculated from the characteristic peaks (001) and (003), which are in good agreement with the published data.[5,6]

Considering the polycrystalline nature of CIGS films with varying x, it is justified that on a macroscopic scale, we take the average values to solve bond length R_{B-Se} in the A_2B_2 tetrahedral clusters around Se for each x, on the basis of the rule of conservation of tetrahedral bonds (CTB)[2,22] in Cu-ternaries. Thus, the R_{B-C} can be described as the covalent bond lengths $R_{III-Se} = (1-x)R_{In-Se} + xR_{Ga-Se}$, and the radii r_B of elemental III are obtained by using Shannon–Perwitt radii[2] from $r_{III} = (1-x)r_{In} + xr_{Ga}$. The nearest-neighbour cation–anion bond lengths R and bond angles θ can be given by using the CTB plus our experimental data η from the following relationships:[2,23]

$$
\begin{aligned}
&R_{Cu-Se} = \left[U^2 + (1+\eta^2)/16\right]^{1/2} a \ \ (\text{nm}),\\
&R_{III-Se} = \left[(U-0.5)^2 + (1+\eta^2)/16\right]^{1/2} a \ \ (\text{nm}),\\
&\theta_{Cu-Se-Cu} = \cos^{-1}\left[1 - 0.25a^2(1+\eta^2)/(2R^2_{Cu-Se})\right] (^\circ),\\
&\theta_{III-Se-III} = \cos^{-1}\left[1 - 0.25a^2(1+\eta^2)/(2R^2_{III-Se})\right] (^\circ),
\end{aligned}
\tag{1}
$$

and the anion displacement parameter U, which reveals the extent of bond alteration in the films, may be calculated by $U = 0.25 + (2+\eta^2)\delta/8 + (2+\eta^2)\delta^3/32 + O(\delta^5)$,[2] by using the mean-square small parameter $\delta \equiv [(r_A + r_{Se})^2 - (r_{III} + r_{Se})^2]/[(r_A + r_{Se})^2 + (r_{III} + r_{Se})^2]$. Figures 2(b) and 3 display the calculated U, R, θ and their fitting curves as a function of x. The values of the bond parameters obtained for $CuInSe_2$, $CuIn_{0.5}Ga_{0.5}Se_2$ and $CuGaSe_2$ are in good agreement with the Refs.[2,24], respectively. It is ob-

served that the U, R and θ with increasing x vary in similar behaviour as that of η. As the U increases from 0.2232 for $CuInSe_2$ to 0.2626 for $CuGaSe_2$, the R_{III-Se} decreases and the R_{Cu-Se} increases, due to In substituted by the smaller atom Ga; meanwhile, the bond angles θ among Cu–Se–III–like configuration (i.e., Cu–Se–Cu and III–Se–III) exhibit corresponding self-adjustment in order to preserve the chalcopyrite structure. This trend parallels the changes in bond charge of Cu–Se and III–Se, for which the increase of the U should weaken the Cu–Se bond and inversely strengthen the III–Se bond, because the U controls the balance between the ionic and covalent contributions to the structure and resultant band gap.[2] And most important, these effects can lead to the interaction among local A_2B_2 clusters with different bond configuration, and consequently give rise to changes in the bond-stretching force constants α and the bond-bending force constants β,[25] which should remarkably affect the Raman frequencies of active modes.

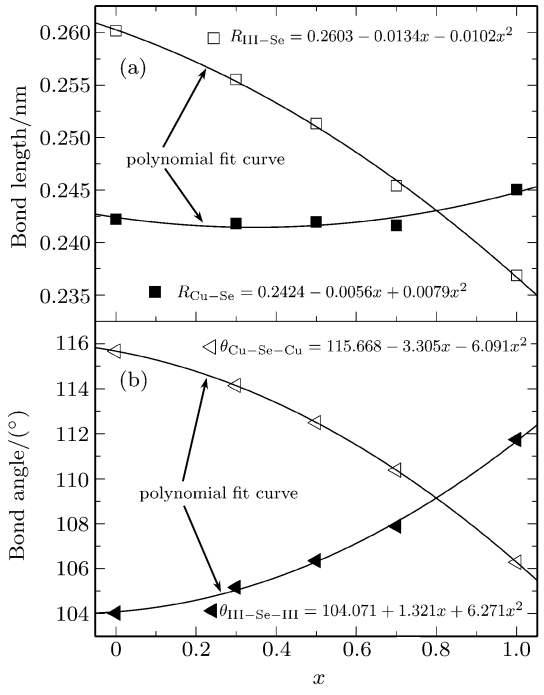


Fig.3. The x dependence of (a) bond length R, and (b) bond angels θ of $CuIn_{1-x}Ga_xSe_2$ films.

3.2. The x dependence of Raman modes in $CuIn_{1-x}Ga_xSe_2$ films

The irreducible representations for the zone-centre Raman active optical modes in the chalcopyrite structure are intensively investigated and expressed as:[4,25] $1A_1+3B_1+3B_2+6E$. The long-range electrostatic interaction causes the splitting of the longitudinal optical and transversal optical high-frequency of B_2 and E modes.

In the following, the main features of our experimental data for CIGS will be presented and briefly discussed, in terms of the bond parameters obtained from the XRD analysis of these films.

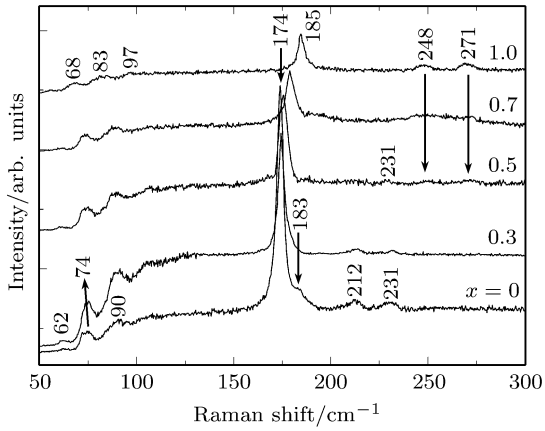


Fig.4. Unpolarized Raman spectra of $CuIn_{1-x}Ga_xSe_2$ films.

3.2.1. The Raman shift of A_1 bands

Figure 4 depicts Raman spectra of CIGS films with x. It is obviously found that the most intense Raman band for $CuInSe_2$ and $CuGaSe_2$ in Fig.4 is the A_1 around 174 and 185 cm^{-1} respectively, in agreement with the previous results.[4,17] This mode corresponds to anion Se movement with cations at rest. According to the force model of Neumann,[25] the frequency of A_1 mode is estimated by

$$v \approx [\alpha_{Cu-Se} + \alpha_{III-Se}/M_{Se}]^{1/2}, \qquad (2)$$

where M_{Se} is the Se mass and α is the cation-Se bond-stretching force constant describing the interaction between nearest neighbours. Moreover, the frequencies of these modes above 150 cm^{-1}[6,16] can be well evaluated by using such empirical approximation method, although neglecting bond-bending force constants β which describe the interaction between second-nearest neighbours.[25]

For CIGS, the frequency of A_1 mode with increasing x is shown in Fig.5(b). The frequency of the A_1 mode in the interval $0 < x < 0.5$ varies slightly with the increase of x and significantly shifts toward higher

wave numbers with $x \geq 0.5$. Over the whole x range, the shift of the A_1 band in CIGS, unlike their lattice constants a and c in Fig.2(a), does not follow the linear Vegard law. The variation of the A_1 mode with x can be obtained by using the polynomial curve

$$A_1\text{Raman shift}(\text{cm}^{-1}) = 173.8 - x + 11.9x^2 \quad (3)$$

with the standard deviation around $0.004\,\text{cm}^{-1}$. Similar behaviour has been observed in the $CuIn_{1-x}Ga_xSe_2$ $(0 \leq x \leq 0.3)$,[8] $Cu(In_{1-x}Ga_x)_3Se_5$ films.[26] For films with $0 \leq x \leq 0.3$, the half width and intensity of the A_1 band change slightly in Fig.4. However, when $x \geq 0.5$, significant broadening and intensity decrease of the A_1 modes should be indicative of presence of the large density of defects due to the enhancement of tetragonal compression ($\eta < 1$), which should lead to degradation in crystalline quality.

Such shift of the A_1 peak depends strongly on the variations of the nearest-neighbour cation–anion bond lengths R with varying x. For the zinc-blende structure (ZB), it is found that the bond-stretching force constants α approximately follow the relation $\alpha = AR^{-n}$,[25,27] where the A and n are constants. Considering the fact that the chalcopyrite structure can be derived from the ZB, in analogy to the analysis of Neumann for the chalcopyrite compounds,[25] it seems justified to suppose that we take this relation to estimate the $\alpha_{\text{Cu-Se}}$ and $\alpha_{\text{III-Se}}$ in CIGS films, using the value[25] $n = 3.01$, as described by the following equations:

$$\begin{aligned}
\alpha_{\text{Cu-Se}} &= A_{\text{Cu-Se}}R_{\text{Cu-Se}}^{-3.01} = [(1-x)A_{\text{Cu-Se}}(CuInSe_2) + xA_{\text{Cu-Se}}(CuGaSe_2)]R_{\text{Cu-Se}}^{-3.01}, \\
\alpha_{\text{III-Se}} &= A_{\text{III-Se}}R_{\text{III-Se}}^{-3.01} = [(1-x)A_{\text{In-Se}}(CuInSe_2) + xA_{\text{Ga-Se}}(CuGaSe_2) - bx(1-x)]R_{\text{III-Se}}^{-3.01}. \quad (4)
\end{aligned}$$

Here, the $A_{\text{Cu-Se}}$ and $A_{\text{In-Se}}$ for $CuInSe_2$ are estimated as 3.675×10^{-28} and $7.904 \times 10^{-28}\,\text{N}\cdot\text{m}^2$ respectively, the $A_{\text{Cu-Se}}$ and $A_{\text{Ga-Se}}$ for $CuGaSe_2$ are calculated as 3.587×10^{-28} and $7.281 \times 10^{-28}\,\text{N}\cdot\text{m}^2$, respectively.

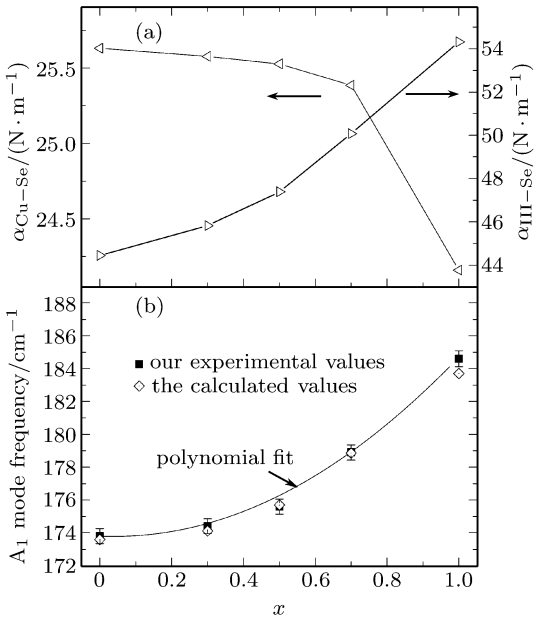


Fig.5. The x dependence of (a) bond-stretching force constants α, and (b) our experimental and the calculated values for A_1 band frequency of $CuIn_{1-x}Ga_xSe_2$ films.

Additionally, the adjustment parameter b in Eq.(4) is given as $b = 100[(1-x)f_{i,\text{In-Se}} + xf_{i,\text{Ga-Se}}] \approx 72$ (the bond ionicity f_i is taken from the Ref.[28]), if the contribution of long-range Coulomb forces to the α[25,27,29] is taken into account, due to the fact[28] that III–Se bond exhibits more ionic than Cu–Se bond. Figure 5(a) depicts the calculated values of the $\alpha_{\text{Cu-Se}}$ and $\alpha_{\text{III-Se}}$ as a function of x, which give the solutions to Eq.(2) shown in Fig.5(b). It is clearly found that the calculated data for the A_1 band are in good agreement with the experimental values. The variation in the anion displacement parameter U should be responsible for the nonlinear shift of the A_1 peak position with x and for the development of intensity of the A_1 band.

3.2.2. The change of Raman mode at 183 cm^{-1}

It is found that a distinct shoulder peak in $CuInSe_2$ is $183\,\text{cm}^{-1}$ in Fig.4. For the films with $x \geq 0.3$, such a shoulder peak becomes almost indiscernible in the noise. The behaviour of the peak in Ga-doped films is obviously different from the A_1 peak for $CuInSe_2$. Considering the sensitive Raman spectra with x, together with the analysis of XRD in this work, we concluded that the band at $183\,\text{cm}^{-1}$ should result from metastable CuAu-ordered $CuInSe_2$ in nominal

chalcopyrite-ordered $CuInSe_2$ other than $CuGaSe_2$, which is identical to the reported experimental results[5,6,16,17] and theoretical prediction.[18,19] According to the recent suggestions by álvarez-García *et al*,[8] such a shoulder peak is assigned to the A_1 mode of CuAu-ordered $CuInSe_2$ phase. To a great extent, the presence of such CuAu-ordered $CuInSe_2$ should be correlated to spontaneous migration and formation of defects (i.e., V_{Cu} and In_{Cu}) controlled by bulk thermodynamics.[3] From our experimental data, it seems justified to suppose that moderate Ga incorporation in $CuInSe_2$ can eliminate metastable CuAu-ordered phase via engineering of compositionally induced local variations in the films,[13] which deserves a further investigation. Phenomenological studies[16] have shown that the formation of CuAu-ordered metastable domains in dominant chalcopyrite-ordered $CuInS_2$ films is related to a deterioration of device performance.

3.2.3. Evolutionary history of Raman bands between 200 and 271 cm^{-1}

With varying x from $CuInSe_2$ to $CuGaSe_2$, the positions and intensities of those peaks between 212 and 271 cm^{-1} are distinctly changed in Fig.4. For the film with $x > 0$, the peaks related to In–Se vibration at 212 and 231 cm^{-1} are weakened, accompanied by the presence of the weaker features at 248 and 271 cm^{-1} for local Ga–Se vibration. For the films with $x \geq 0.5$, the intensity of two peaks at 248 and 271 cm^{-1} is gradually enhanced.

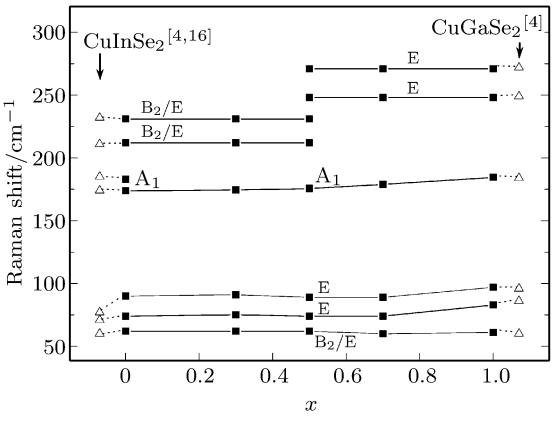


Fig.6. The composition dependence of the phonon frequencies of different vibration modes in $CuIn_{1-x}Ga_xSe_2$ films. The solid squares correspond to the $CuInSe_2$-like and $CuGaSe_2$-like modes in this work, additionally, the triangles denote data in Refs.[4,16] (lines are guides for the eye only). These data follow the analysis of the spectra shown in Fig.4.

These bands in the region between 200 cm^{-1} and 271 cm^{-1} are identified with the end members and exhibited in Fig.6, which shows clearly two-mode behaviour and indicates chalcopyrite phase transition with increasing x. Since the discrepancies between the assignments of Raman modes are usually present in $CuInSe_2$[4–6,16] and $CuGaSe_2$[4,7], the possible assignment for $CuInSe_2$ and $CuGaSe_2$ is proposed on the basis of Refs.[4,16] and [4] respectively. For CIGS films with $0 < x < 1$ in this work, the assignments are mainly based on both the mode assignment of the end members and the shift history of corresponding phonon frequencies in films with x. Figure 6 draws a graphical comparison between all the observed lines in Fig.4 and the data in Refs.[4,16].

3.2.4. One-mode behaviour in the low-frequency region below 100 cm^{-1}

For the low-frequency modes E and B_2 at 62, 74 and 90 cm^{-1} in $CuInSe_2$, their intensities are slightly changed with $x \leq 0.7$ and their frequencies shift within 3 cm^{-1}, whereas, these three peaks are around 68, 83 and 97 cm^{-1} in $CuGaSe_2$. Such continuous shift exhibits one-mode behaviour. Unlike the high-frequency bands mainly affected by cation-Se bonds, the two modes are mainly ascribed to the bond-bending force constants β of Cu-Se-III (or III-Se-III, Cu-Se-Cu, etc.) configuration, which are mainly determined by the interaction between bond angles θ around it nearby,[6] and they depend weakly on anion mass.[25,30] As x increases, the variations of $\theta_{III-Se-III}$ and $\theta_{Cu-Se-Cu}$ in Fig.3(b) behave similarly as that of the anion displacement parameter U, which should affect the shift of E and B_2 modes. The low-frequency bands in this work are slightly different from that in the bulky crystal,[4] because the strain due to the lattice mismatch and the thermal expansion coefficients of substrate (glass) in our 60 nm films are not fully relaxed (a critical thickness of 120 nm[7]) yet.

4. Conclusions

The effects of Ga content x on structural properties of $CuIn_{1-x}Ga_xSe_2$ films have been systematically investigated by Raman scattering and x-ray diffraction spectra. From the evolutionary history of Raman spectra with x, it is found that the shift of the dominant A_1 mode, unlike the lattice constants, exhibits approximately polynomial change but not lin-

ear curve, and moderate Ga incorporation in $CuInSe_2$ can effectively eliminate the metastable CuAu-ordered phase. The low frequencies below 100 cm^{-1} show one-mode behaviour, whereas, the high frequencies in the region between 200 and 272 cm^{-1} exhibit clearly two-mode behaviour. From the analysis of the experimental data in this work, we establish a semiquantitative relationship among Raman A_1 shift, x and the anion displacement parameter U. Additionally, on a macroscopic scale, the bond parameters of the lattice are calculated as a function of Ga content x. Comparing our experimental data with the reported data of the related compounds, together with the data calculated from the force model of Neumann, we explain the composition-induced structural modifications in quaternary CIGS films. The variations of bond-bending force constants in CIGS films, and the evolution of CuAu-ordered $CuInSe_2$ in low Ga-containing films, need a further investigation.

Acknowledgments

One of the authors (Xu Chuan-Ming) gratefully acknowledges Professor Xu Cun-Yi from the Structure Research Laboratory of Chinese Academy of Sciences for the sample measurements.

References

[1] Persson C and Zunger A 2005 *Appl. Phys. Lett.* **87** 211904
[2] Jaffe J E and Zunger A 1984 *Phys. Rev.* B **29** 1882
[3] Zhang S B, Wei S H, Zunger A and Katayama-Yoshita H 1998 *Phys. Rev.* B **57** 9642
[4] Rincón C, Wasim S M, Marín G, Delgado J M, Huntzinger J R, Zwick A and Gabibert J 1998 *Appl. Phys. Lett.* **73** 441
[5] Stanbery B J, Kincal S, Kim S, Chang C H, Ahrenkiel S P, Lippold G, Neuman H, Anderson T J and Crisalle O D 2002 *J. Appl. Phys.* **91** 3598
[6] Łażewski J, Neumann H, Parlinski K, Lippold G and Stanbery B J 2003 *Phys. Rev.* B **68** 144108
[7] Xue C, Papadimitriou D, Raptis Y S, Esser N, Richter W, Siebentitt S and Lux-Steiner M C 2003 *J. Appl. Phys.* **94** 4341
[8] Xu C M, Xu X L, Min H J, Xu J, Yang X J, Huang W H and Liu H T 2003 *Chin. J. Semicond.* **24** 1057
[9] Bodnar I V, Smirnova G F, Smirnova T V, Aleshchenko A and Vodopyanov L K 1988 *Phys. Stat. Sol.* B **145** 117
[10] Tanino H, Deai H and Nakanish H 1993 *Jpn. J. Appl. Phys. Suppl.* **32**–**33** 436
[11] Wei S H, Zhang S B and Zunger A 1998 *Appl. Phys. Lett.* **72** 3199
[12] Persson C and Zunger A 2003 *Phys. Rev. Lett.* **91** 266401
[13] Yan Y F, Noufi R, Jones K M, Ramanathan K, Al-Jassim M M and Stanbery B J 2005 *Appl. Phys. Lett.* **87** 121904
[14] Zhang S B and Wei S H 2002 *Phys. Rev.* B **65** 081402
[15] Contreras M A, Egass B, King D, Swartzlander A and Dullweber T 2000 *Thin Solid Films* **361**–**362** 167
[16] Álvarez-García J, Barcones B, Pérez-Rodrgíuez A, Romano-Rodrgíuez A, Morante J R, Janotti A, Wei S H and Scheer R 2005 *Phys. Rev.* B **71** 054303
[17] Xu C M, Xu X L, Xu J, Yang X J, Zuo J, Kong N, Huang W H and Liu H T 2004 *Semicond. Sci. Technol.* **19** 1201
[18] Wei S H, Zhang S B and Zunger A 1999 *Phys. Rev.* B **59** R2478
[19] Su D S and Wei S H 1999 *Appl. Phys. Lett.* **74** 2483
[20] El Haj Moussa G W, Ajaka M, El Tahchi M, Eid E and Llinares C 2005 *Phys. Stat. Sol.* A **202** 469
[21] Rincón C, Wasim S M, Marín G, Delgado J M and Contreras J 2003 *Appl. Phys. Lett.* **83** 1328
[22] Jaffe J E and Zunger A 1983 *Phys. Rev.* B **27** 5176
[23] Garbato L, Ledda F and Rucci A 1987 *Prog. Cryst. Growth and Charact.* **15** 1
[24] Díaz R, Martín T, Merino J M, León M, Martín de idales J L and Rueda F 2000 *J. Appl. Phys.* **88** 1776
[25] Neumann H 1985 *Helv. Phys. Acta* **58** 337
[26] Xu C M, Xu X L, Xu J, Yang X J, Zuo J, Dang X M, Feng Y, Huang W H and Liu H T 2004 *Chin. J. Semicond.* **25** 1423
[27] Martin R M 1970 *Phys. Rev.* B **1** 4005
[28] Xue D, Betzler K and Hesse A 2000 *Phys. Rev.* B **62** 13546
[29] Sun W L and Li Z M 2000 *Chin. Phys.* **9** 445
[30] Huang S H and Mo Y D 2001 *Acta Phys. Sin.* **50** 964 (in Chinese)